

Optimization Design of Cementitious Materials Based on Molybdenum Tailings-Desulfurization Gypsum-Calcium Carbide Sludge

Ziru Guo, Haijie Li, Shiyong Chen *

College of Resources and Environment, Henan Polytechnic University, Jiaozuo 454003, China

ABSTRACT

This study developed a composite cementitious material using molybdenum tailings, desulfurization gypsum, and carbide slag as the primary raw materials. The appropriate dosage range of each component was first determined through single-factor experiments. The mix proportion was then optimized using an orthogonal experimental design, and a strength prediction model was established via response surface methodology. The microstructure and hydration mechanism were further investigated by XRD and SEM. The results indicate that the optimal mix ratio is molybdenum tailings: desulfurization gypsum: carbide slag = 29.66 g: 35.45 g: 45 g, with a water-to-binder ratio of 0.402. The 28-day compressive strength of the prepared cementitious material reached 5.59 MPa. The main hydration products were ettringite (AFt) and C-S-H gel, which interweave to form a dense microstructure. This system demonstrates a high-value approach to recycling solid waste and offers a sustainable strategy for producing eco-friendly cementitious materials.

KEYWORDS

Molybdenum tailings; Desulfurization gypsum; Carbide slag; Cementitious material; Response surface optimization; Hydration mechanism

1. INTRODUCTION

With the continuous exploitation and utilization of mineral resources, progressive depletion and declining ore grades have become pressing issues [1]. The large quantities of tailings generated from mineral processing operations not occupy land and cause soil and water pollution [2], but also increase the costs associated with the construction and maintenance of tailings reservoirs. Moreover, they pose significant safety and environmental risks to surrounding ecosystems and communities [3, 4]. The comprehensive utilization of tailings resources has thus attracted worldwide attention. Converting waste into valuable materials, mitigating hazards, saving land, and benefiting society are demands of economic development as well as environmental protection. Therefore, the resource recovery, volume reduction, and detoxification of tailings—achieving “zero tailing” through comprehensive utilization—represent an effective strategy to eliminate the hazards posed by tailings accumulation [5]. This approach not only enhances the economic efficiency of mining enterprises but also contributes positively to social development and environmental sustainability.

As a major waste product generated from molybdenum mining and beneficiation processes [6], molybdenum tailings pose critical challenges to sustainable mining development due to environmental concerns and resource wastage associated with their long-term storage. These tailings contain valuable metallic elements as well as non-metallic minerals such as quartz and feldspar [7]. When exposed to open-air conditions, rainwater leaching can facilitate the migration of heavy metals, leading to contamination of soil and groundwater systems, and thereby threatening both ecological

security and human health [8]. Meanwhile, the global construction industry's heavy reliance on conventional cement contributes significantly to the depletion of limestone resources and increased carbon emissions [9], which contradicts the strategic objectives of the "Dual Carbon" initiative. Therefore, developing novel green and low-carbon cementitious materials derived from industrial solid waste [10] represents not only an urgent solution to mitigate environmental risks from tailings but also an essential pathway for the green transformation of the building materials sector. Desulfurization gypsum and carbide slag, by-products from thermal power and chemical industries, also face challenges in large-scale disposal owing to their high impurity content and low utilization rates [11, 12]. In the context of China's "Dual Carbon" strategy and the development of "Zero-Waste Cities", promoting the synergistic and resourceful utilization of industrial solid wastes has emerged as a crucial approach to alleviating environmental constraints [13].

Currently, the application of molybdenum tailings (MT) in cementitious materials is predominantly focused on their use as auxiliary supplementary materials, with limited research on their utilization as a primary component. Luo [14] prepared concrete using a composite binder composed of MT, fly ash, and cement. Their findings revealed that in the later hydration stage of the MT-based cementitious system, the main products—C–S–H gel and ettringite (AFt)—interwove with other hydration products. Additionally, fine unreacted particles filled the pores of the system, thereby enhancing the compressive strength of the concrete. Yu Xiaojun [15] investigated the effects of MT powder as a supplementary material on cement-based systems. They observed that when 30% of cement was replaced by MT powder, the internal structure of the paste became denser. Besides hydration products such as ettringite and calcium hydroxide, minerals originally present in the MT powder, including SiO₂, feldspar, and mica, were also identified in the paste. Wang [16] proposed a low-carbon preparation method involving the synergistic replacement of both cementitious material and fine aggregate with molybdenum tailings waste (MTW). Their study demonstrated that appropriate incorporation of MTW could improve pore structure, enhance the interfacial transition zone (ITZ), and increase carbonation resistance. Due to the low comprehensive utilization rate of desulfurization gypsum (DG) and carbide slag (CS), researchers have also conducted related studies. Cui [17] activated phosphorous slag synergistically using CS and DG. They found that CS could activate the pozzolanic activity of the slag to form C–S–H gel, while the addition of DG and metakaolin promoted the formation of abundant AFt, C–S–H, and stratlingite. Qi Guangzheng [18] investigated the effect of DG content on the hydration characteristics of calcium aluminate–carbide slag co-activated supersulfated cement. Their results indicated that during early hydration, DG rapidly reacted with calcium aluminate to form ettringite, while CS provided an alkaline environment that facilitated the dissolution of slag. In the later hydration stages, calcium silicate hydrate (C–S–H) gradually became the dominant hydration product, contributing to the continuous development of matrix strength. Ji [19] developed a cementitious material using ground granulated blast furnace slag (GGBS), CS, and DG. They reported that CS provided an alkaline environment promoting the dissolution of GGBS and the formation of C–A–S–H gel, while DG supplied SO₄²⁻ for the formation of AFt.

The complementary composition of molybdenum tailings (MT), desulfurization gypsum (DG), and carbide slag (CS) offers a natural basis for the preparation of cementitious materials. MT is rich in reactive silicon and aluminum components, DG serves as a source of sulfate activation, and CS provides a calcium-based alkaline environment [20]. Together, these components synergistically form a non-fired, low-carbon cementitious system, enabling the high-value conversion of all solid waste components. From a techno-economic perspective, this material employs ambient temperature curing without the need for high-temperature sintering, leading to significantly reduced carbon emissions compared to conventional cement production [21]. Moreover, the raw material cost is reduced by 30% to 50% due to the large-scale substitution of solid wastes, making the material both low-carbon and economically competitive. In summary, research on the development of cementitious materials from molybdenum tailings originates from environmental concerns and aims at resource utilization of solid wastes and the production of low-carbon building materials [22]. It carries notable

scientific value [23], ecological benefits, and industrial potential, representing an important research direction for promoting the sustainable integration of the mining and construction materials industries. This study utilizes three types of industrial solid wastes—molybdenum tailings, desulfurization gypsum, and carbide slag—to fabricate a novel composite cementitious material. In this system, desulfurization gypsum acts as both a calcium source and a sulfate activator, while carbide slag serves as a calcium source and an alkaline activator [24]. The combined use of these wastes not only provides a new strategy for producing green cementitious materials but also enables large-scale valorization of industrial by-products, mitigating their environmental impact. This approach possesses considerable practical significance and scientific value.

2. EXPERIMENTAL SECTION

2.1. Raw Materials

The molybdenum tailings used in this study were collected from the tailings reservoir of a molybdenum mine in Luonan, Henan Province. Desulfurization gypsum was obtained from Henan Huarun Power Shouyangshan Co., Ltd., and carbide slag was sourced from Henan Energy and Chemical Industry Group Hebi Coal Chemical Co., Ltd. The chemical compositions of the raw materials were analyzed using X-ray fluorescence (XRF) spectrometry, and the results are presented in Table 1-1.

Table 1-1. Chemical composition of raw materials (w/%)

Types	SiO ₂	Al ₂ O ₃	SO ₃	Na ₂ O	K ₂ O	Fe ₂ O ₃	CaO	MgO
Molybdenum	32.50	11.63	5.56	3.35	2.12	39.96	1.40	—
Desulfurization gypsum	0.02	0.01	56.15	0.07	—	—	43.56	0.09
Calcium carbide slag	1.59	0.67	0.43	0.28	0.03	0.26	95.79	0.78

As shown in Table 1-1, the primary chemical components of molybdenum tailings are SiO₂, Al₂O₃, and Fe₂O₃. Desulfurization gypsum consists mainly of SO₃ and CaO, while carbide slag is predominantly composed of CaO.

The phase composition of the molybdenum tailings was analyzed using X-ray diffraction (XRD). A small amount of the sample was ground and passed through a 200-mesh sieve prior to XRD measurement. The results are presented in Figure 1-1.

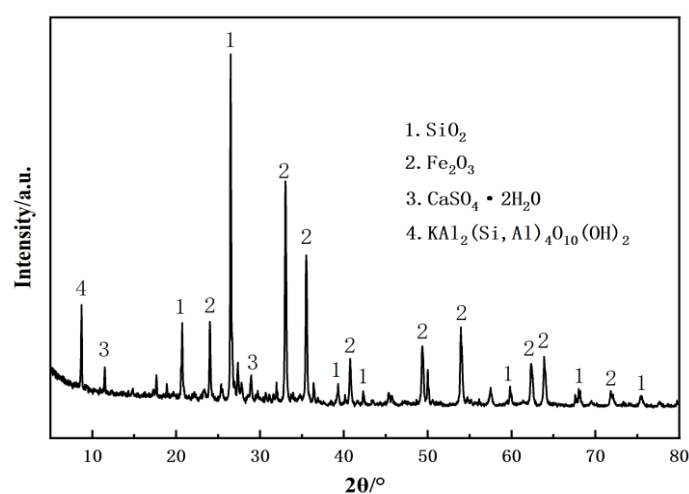


Figure 1-1. XRD pattern of molybdenum tailings

As shown in Figure 1-1, the molybdenum tailings are primarily composed of quartz (SiO₂) and hematite (Fe₂O₃), with other compounds such as mica present in minor amounts. Silicon is mainly

found in the form of quartz. Quartz, a silicate mineral with high crystallinity and chemical stability, contributes to the relatively low pozzolanic activity of the molybdenum tailings.

2.2. Experimental Design

An L9 (three-factor, three-level) orthogonal experimental design was employed [25]. The three factors consisted of the dosage of molybdenum tailings (A), the dosage of desulfurization gypsum (B), and the dosage of carbide slag (C). The water-to-binder ratio was fixed at 0.4. The specific level values for each factor are presented in Table 1-2.

Table 1-2. The various factors and levels of orthogonal experiments

Level	Corresponding value of the level%		
	A	B	C
1	25	25	40
2	35	30	45
3	45	35	50

A response surface methodology (RSM) experiment was designed using the Box–Behnken design (BBD) approach [26]. The three independent variables selected were the mass ratio of molybdenum tailings to carbide slag (denoted as m(MoT/CS)), the mass ratio of desulfurization gypsum to carbide slag (denoted as m(DG/CS)), and the water-to-binder ratio (denoted as W/B). The compressive strength of the cementitious system at 3, 7, and 28 days was set as the response variable. The design included five center points. The factor-level coding table for the response surface design is shown in Table 1-3, where -1, 0, and 1 represent the low, middle, and high levels of each factor, respectively [27].

Table 1-3. A comparison table of factor levels for response surface design

Encoded value	Factors and corresponding levels		
	m (MoT/CS) (%)	m (DG/CS) (%)	W/B
-1	55.6	66.7	0.35
0	66.7	77.8	0.40
1	77.8	88.9	0.45

In the mixture proportion design, after testing the performance responses at various experimental points corresponding to different factor combinations, the response surface function was fitted using the least squares method [28]. A standard polynomial regression was applied to the data, resulting in a second-order polynomial equation. This equation serves as the model describing the relationship between compressive strength and the various mineral admixtures [29], as expressed by Equation (1).

$$Y = \beta_0 + \sum_{i=1}^K \beta_i X_i + \sum_{i=1}^K \beta_{ii} X_i^2 + \sum_{i < j}^K \beta_{ij} X_i X_j + \varepsilon \quad (1)$$

Where Y is the predicted response value; β_0 , β_i , and β_{ii} represent the constant term, the linear coefficient, and the quadratic coefficient, respectively; β_{ij} denotes the interaction coefficient between factors; X_i and X_j are the coded levels of the independent variables; ε is the random error; and K is the number of independent variables.

2.3. Experimental Method

The chemical composition of the raw materials was analyzed using a Bruker S8 TIGER X-ray fluorescence (XRF) spectrometer [30]. Phase composition of the samples was examined by X-ray

diffraction (XRD, Rigaku Ultima IV) [31] under the following conditions: Cu K α radiation ($\lambda = 1.541 \text{ \AA}$), 40 kV voltage, 40 mA current, a scanning range (2θ) of 5° to 80° , a step size of 0.02° , and a scanning speed of $10^\circ/\text{min}$. To terminate hydration, the samples were immersed in anhydrous ethanol, dried at 50°C until constant weight was achieved, ground into powder, and then subjected to XRD analysis. Microstructure and elemental distribution were characterized using scanning electron microscopy coupled with energy-dispersive spectroscopy (SEM-EDS, Merlin Compact).

2.4. Preparation of Gelling Material

The solid raw materials, including molybdenum tailings, desulfurization gypsum, and carbide slag, were precisely weighed according to the predetermined ratios from parallel experiments and thoroughly blended. The mixture was then transferred into a JJ-5 planetary mixer and dry-mixed at low speed for 40 seconds. A predetermined mass of water was subsequently added along the inner wall of the mixing bowl. The wet mixing process consisted of a low-speed phase for 80 seconds, followed by a high-speed phase for 2 minutes. The resulting paste was cast into $40 \text{ mm} \times 40 \text{ mm} \times 160 \text{ mm}$ triple-gang molds according to the Chinese National Standard GB/T 17671-2021 (equivalent to the ISO method for testing the strength of cement mortar). The molds were then placed on a vibrating table to ensure a uniform and compact slurry. After being cured at room temperature for 24 hours, the specimens were demolded. Subsequently, they were subjected to natural curing until the designated testing ages were reached.

3. RESULTS AND DISCUSSION

3.1. Orthogonal Experiment Results

In accordance with the orthogonal experimental design, compressive strength tests were conducted on the composite cementitious material at ages of 3, 7, and 28 days. The results of the orthogonal experiments for the molybdenum tailings–desulfurization gypsum–carbide slag composite cementitious system are presented in Table 2-1.

Table 2-1. Strength test scheme and results of molybdenum tailings–desulfurization gypsum–calcium carbide slag composite cementitious material

Serial number	Dosage/g			Compressive strength/MPa		
	Molybdenum tailings	Desulfurization gypsum	Calcium carbide slag	3 d	7 d	28 d
A1	25	25	40	0.72	1.48	2.90
A2	25	30	45	0.71	1.52	2.80
A3	25	35	50	0.75	1.57	2.92
A4	35	25	45	0.67	1.4	2.85
A5	35	30	50	0.66	1.46	3.06
A6	35	35	40	0.6	1.41	3.16
A7	45	25	50	0.5	1.4	2.68
A8	45	30	40	0.53	1.23	2.98
A9	45	35	45	0.45	1.31	2.69

3.2. Range Analysis and Analysis of Variance

The range analysis and analysis of variance results for the molybdenum tailings–desulfurization gypsum–carbide slag composite cementitious material are summarized in Table 2-2 and Table 2-3, respectively.

Table 2-2. Range analysis results

Type	Indicator	Molybdenum tailings (A)	Desulfurization gypsum (B)	Calcium carbide slag (C)	Significance
R _{3d} /MPa	k ₁	0.727	0.630	0.617	A>B>C
	k ₂	0.643	0.633	0.610	
	k ₃	0.493	0.600	0.637	
	Extremely poor	0.233	0.033	0.027	
	Optimal level	A ₁	B ₂	C ₃	
R _{7d} /MPa	k ₁	1.523	1.427	1.373	A>C>B
	k ₂	1.423	1.403	1.410	
	k ₃	1.313	1.430	1.477	
	Extremely poor	0.210	0.027	0.103	
	Optimal level	A ₁	B ₃	C ₃	
R _{28d} /MPa	k ₁	2.873	2.810	3.013	A>C>B
	k ₂	3.023	2.947	2.780	
	k ₃	2.783	2.923	2.887	
	Extremely poor	0.240	0.137	0.233	
	Optimal level	A ₂	B ₂	C ₁	

At the curing age of 3 days, the range values for each factor were 0.2333, 0.033, and 0.027, respectively, indicating that the order of influence on compressive strength was: molybdenum tailings content > desulfurization gypsum content > carbide slag content. At 7 days, the corresponding range values were 0.210, 0.027, and 0.103, suggesting the order of influence as: molybdenum tailings content > carbide slag content > desulfurization gypsum content. By 28 days, the range values obtained were 0.240, 0.137, and 0.233, which demonstrated that the order of influence on the 28-day compressive strength was: molybdenum tailings content > carbide slag content > desulfurization gypsum content.

Table 2-3. Analysis of Variance results

Time	Raw materials	DF	Adj SS	Adj MS	F	P	Significance
3 d	Molybdenum tailings (A)	2	0.084	0.042	21.95	0.044	A>B>C
	Desulfurization gypsum (B)	2	0.002	0.001	0.53	0.654	
	Calcium carbide slag (C)	2	0.001	0.001	0.3	0.768	
7 d	Molybdenum tailings (A)	2	0.066	0.033	23.09	0.042	A>C>B
	Desulfurization gypsum (B)	2	0.001	0.001	0.44	0.694	
	Calcium carbide slag (C)	2	0.016	0.008	5.74	0.148	
28 d	Molybdenum tailings (A)	2	0.088	0.044	35.76	0.027	A>C>B
	Desulfurization gypsum (B)	2	0.032	0.016	13.00	0.071	
	Calcium carbide slag (C)	2	0.082	0.041	33.19	0.029	

Based on the range and variance analysis results, the optimal mix proportion for 3-day compressive strength was identified as A₁B₂C₃, corresponding to molybdenum tailings : desulfurization gypsum : carbide slag =25:30:50. For 7-day strength, the optimal combination was A₁B₃C₃, with a mass ratio of 25:35:50. At 28 days, the best performance was achieved with combination A₂B₂C₁, representing a proportion of 35:30:40.

3.3. Experimental Results of the Response Surface

Table 2-4. Experimental results of response surface design

Serial number	m (MoT/CS)/%	m (DG/CS)/%	W/B	Compressive strength/Mpa		
				3d	7d	28d
1	66.7	77.8	0.4	0.92	1.78	5.03
2	55.6	88.9	0.4	0.78	1.24	2.96
3	55.6	77.8	0.35	0.67	1.16	2.93
4	66.7	77.8	0.4	0.91	1.83	5.07
5	66.7	88.9	0.35	0.75	1.55	4.05
6	77.8	66.7	0.4	0.62	1.2	2.05
7	66.7	77.8	0.4	0.94	1.84	4.94
8	77.8	88.9	0.4	0.66	1.48	2.58
9	77.8	77.8	0.45	0.58	1.56	2.05
10	55.6	66.7	0.4	0.63	1.01	3.37
11	66.7	77.8	0.4	0.93	1.75	4.99
12	66.7	88.9	0.45	0.52	1.47	2.16
13	66.7	77.8	0.4	0.99	1.87	4.88
14	66.7	66.7	0.35	0.53	1.08	1.95
15	77.8	77.8	0.35	0.82	1.44	4.17
16	66.7	66.7	0.45	0.65	1.6	3.38
17	55.6	77.8	0.45	0.83	1.62	4.61

3.4. Response Surface Model Analysis

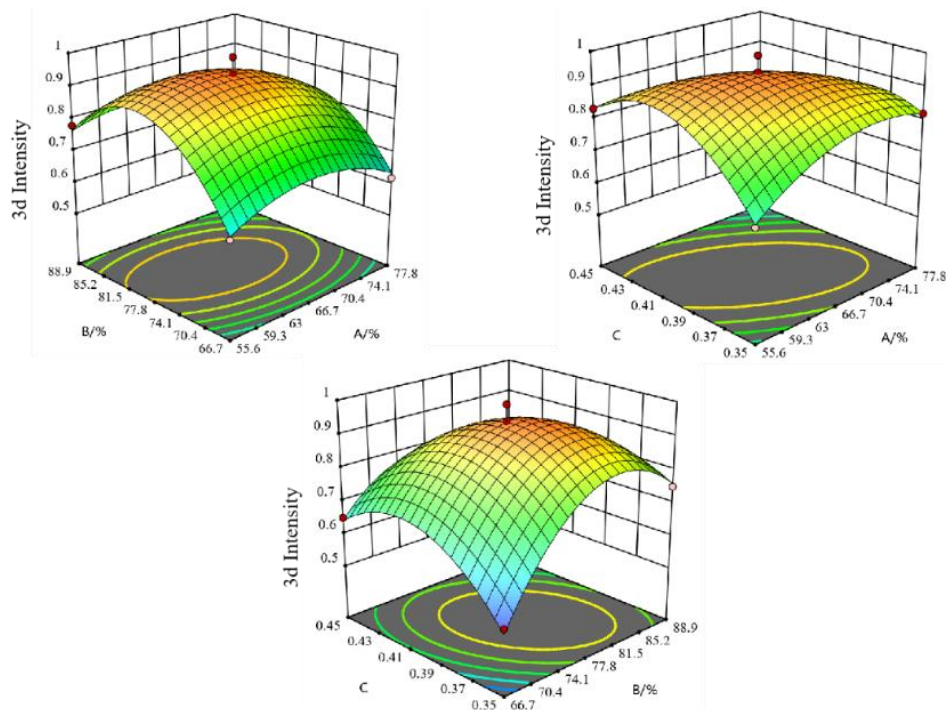


Figure 2-1. 3d response diagram of the composite system at 3D age

Figure 2-1 shows the three-dimensional response surface plot of the composite system at 3 days of curing. When the water-to-binder ratio (W/B) was fixed, the interaction between m (MoT/CS) and m (DG/CS) was limited. The main reason is that molybdenum tailings primarily govern the silicate polycondensation reaction, while desulfurization gypsum dominates sulfate activation. These two processes occur largely in parallel during the early hydration stage, resulting in weak synergism. When

m (DG/CS) was held constant, a pronounced interactive effect was observed between m (MoT/CS) and W/B. The water-to-binder ratio directly influences the pozzolanic reaction efficiency of the silicon-aluminum phases in the molybdenum tailings by controlling ionic diffusion rates and reactant dissolution equilibrium. Simultaneously, the proportion of molybdenum tailings modulates the water demand of the system. This dynamic interdependence leads to a significant interaction. When m (MoT/CS) was fixed, a strong interaction was also identified between m (DG/CS) and W/B. The response surfaces for the 3-day curing period exhibit a distinct downward-opening curvature with clear maximum points, indicating that an optimal combination of factor levels exists within the experimental range.

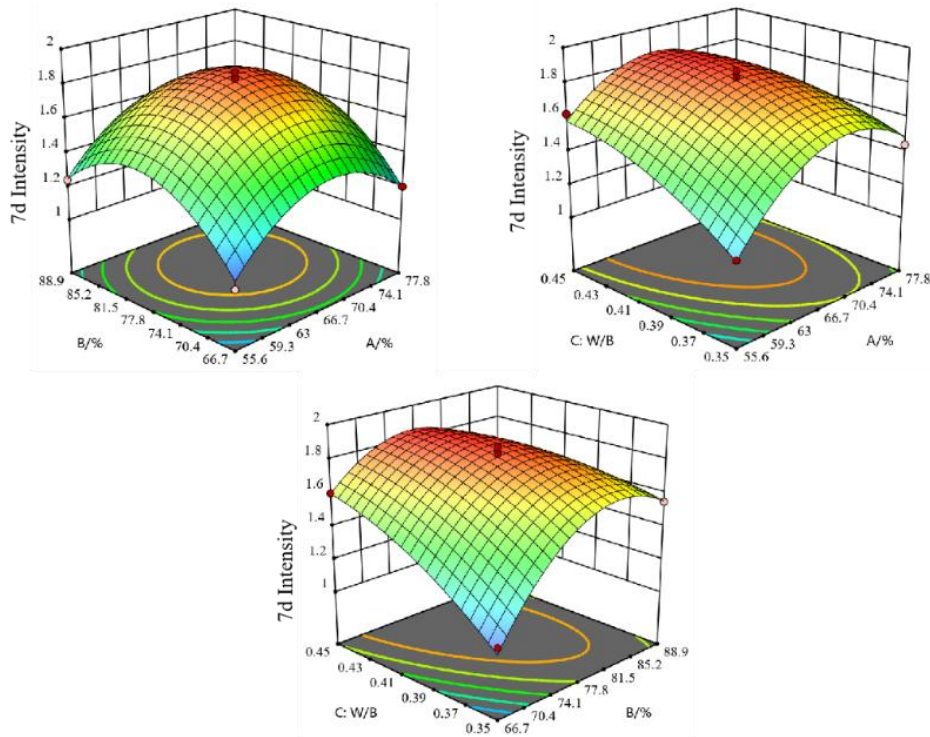


Figure 2-2. 7d response diagram of the composite system at 3D age

Figure 2-2 presents the three-dimensional response surface plot for the composite system after 7 days of curing. The experimental results indicate that clear optimal proportion intervals exist for the two-factor interactions of AB, AC, and BC. An excessively high or low ratio of any two components resulted in a reduction in cementitious strength. At 7 days of curing, the water-to-binder ratio (W/B) emerged as the key factor influencing performance. An increase in water content enhanced the utilization efficiency of both molybdenum tailings and desulfurization gypsum, leading to a simultaneous increase in their optimal proportions. This can be attributed to the fact that sufficient moisture promotes the dissolution of reactive components from the molybdenum tailings, facilitating the formation of gel products, while also improving the dispersion of gypsum, thereby supporting a more homogeneous development of the strength-forming microstructure.

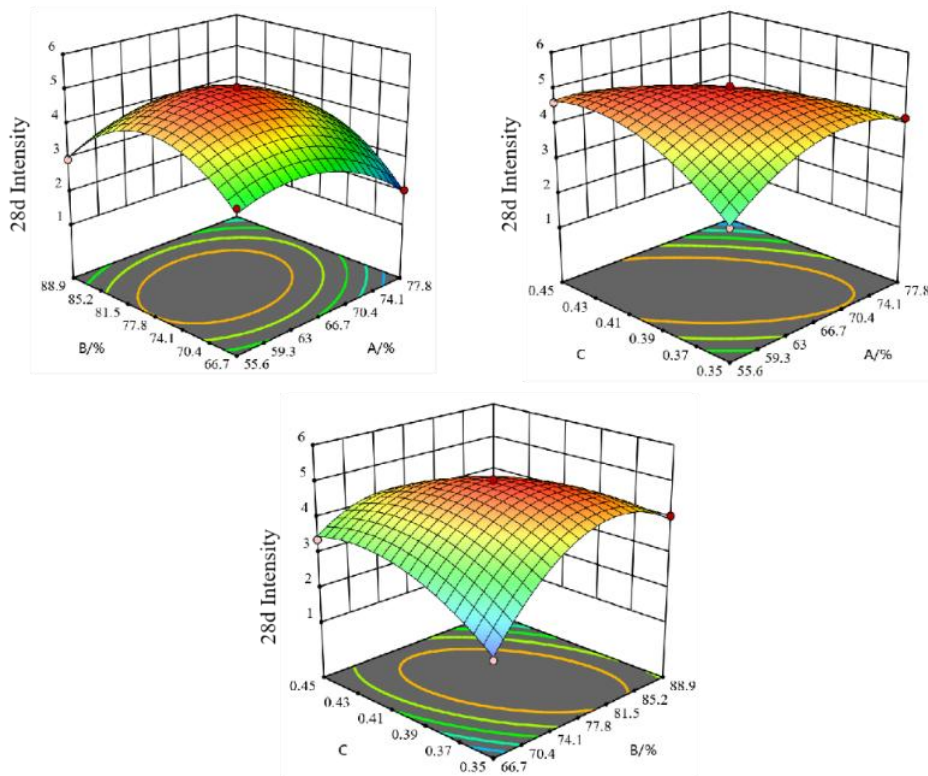


Figure 2-3. 28d response diagram of the composite system at 3D age

Figure 2-3 shows the three-dimensional response surface plot of the composite system after 28 days of curing. Following the 28-day curing period, the interaction between factors A and B (m (MoT/CS) and m (DG/CS)) was significant, with strength initially increasing and then decreasing as their ratios rose, indicating the presence of an optimal synergy point beyond which performance declines. In contrast, the interactions AC and BC were highly significant. Under sufficient moisture conditions, the active components in the molybdenum tailings were continuously released, forming a dense C–S–H gel, resulting in a steady increase in strength with higher factor A (m (MoT/CS)). Meanwhile, desulfurization gypsum contributed to strength development by forming ettringite (AFt) to refine the pore structure. However, excessive water content increased the porosity of the paste, thereby diminishing the enhancing effect provided by the gypsum.

3.5. Response Surface Optimization And Verification

Through multi-objective optimization using response surface methodology, the mixture proportions of the composite cementitious system were optimized with the goal of maximizing the response values. The optimal ratios under 3-, 7-, and 28-day curing conditions were determined as follows: m (MoT/CS) = 65.909, m (DG/CS) = 78.786, and W/B = 0.402. This corresponds to the mass proportions of molybdenum tailings: desulfurization gypsum: carbide slag = 29.66 g: 35.45 g: 45 g, with a water-to-binder ratio of 0.402. Furthermore, the experimental results showed that the relative errors between the measured and predicted compressive strengths at 3, 7, and 28 days were 3.97%, 3.55%, and 4.29%, respectively, all of which are below 5%. This indicates that the developed response surface model possesses good predictive accuracy, and the optimization results are reliable, demonstrating a high degree of precision.

3.6. Phase Composition Analysis

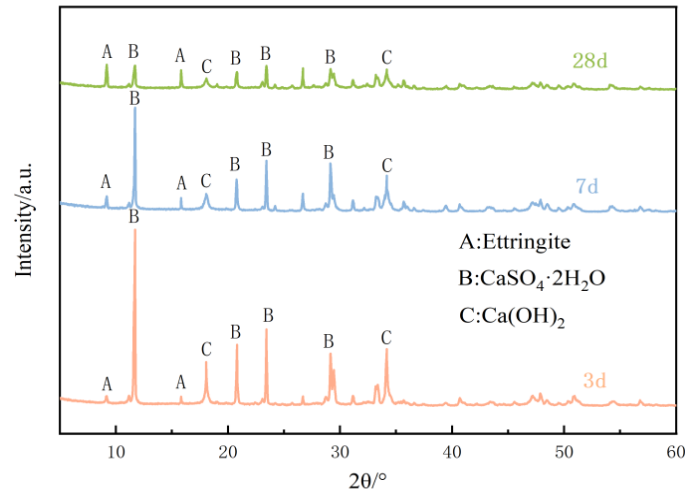


Figure 2-4. XRD patterns of samples at different ages

Figure 2-4 shows the XRD patterns of the cementitious samples hydrated for 3, 7, and 28 days under the optimal mix proportion determined by the response surface experiment. It can be observed that at 3 days of curing, a significant amount of unreacted gypsum and carbide slag remained in the system. As the curing age increased, the characteristic peaks of these two components gradually weakened and almost disappeared by 28 days, indicating their near-complete consumption through hydration reactions. Furthermore, distinctive peaks of ettringite (AFt) were detected after 3 days and progressively intensified with prolonged curing, demonstrating a continuous formation of AFt throughout the hydration process.

3.7. Microscopic Morphology Analysis

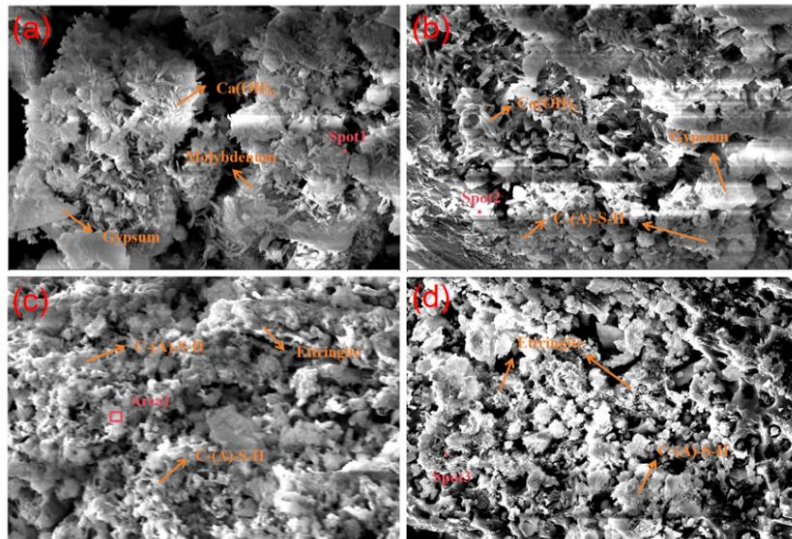


Figure 2-5. SEM images of the curing of cementitious materials for 3 days, 7 days and 28 days

As shown in the corresponding figures, at 3 days of curing (Figure a), a considerable amount of $\text{Ca}(\text{OH})_2$ and $\text{CaSO}_4 \cdot 2\text{H}_2\text{O}$ was observed adhering to the surface of molybdenum tailings. The internal structure of the system was loose with large pores at this stage. By 7 days of curing (Figure b), the content of $\text{Ca}(\text{OH})_2$ and $\text{CaSO}_4 \cdot 2\text{H}_2\text{O}$ decreased, indicating their participation in the reaction. The formation of some C-(A)-S-H gel was also noted, leading to a denser structure. After 28 days of curing (Figures c and d), abundant C-(A)-S-H gel and ettringite were formed, interconnecting and

bonding tightly. No $\text{Ca}(\text{OH})_2$ or $\text{CaSO}_4 \cdot 2\text{H}_2\text{O}$ was detected, suggesting their near-complete consumption. The gel matrix appeared compact and continuous, with no significant pores observed.

4. CONCLUSION

(1) The optimal mix proportion for the cementitious material prepared from molybdenum tailings, desulfurization gypsum, and calcium carbide residue was determined as follows: molybdenum tailings : desulfurization gypsum : calcium carbide residue = 29.66g:35.45g:45g, with a water-to-binder ratio of 0.402.

(2) The primary hydration products of the molybdenum tailings–desulfurization gypsum–calcium carbide residue composite cementitious system were identified as C–S–H gel and AFt. With prolonged curing age, the content of hydration products increased gradually. The interwoven growth of C–S–H gel and AFt crystals contributed to a reduction in the internal porosity of the specimens, thereby promoting the development of mechanical strength.

(3) In this system, desulfurization gypsum serves as both a calcium source and a sulfate activator, while calcium carbide residue acts as a calcium source and an alkaline activator. The synergistic use of these three raw materials offers a novel approach for developing sustainable cementitious materials, providing new insights into the production of green binders.

REFERENCES

- [1] Yuan, L., Wang, X., Qi, M., et al. Research progress on the preparation of adsorbent materials from mine tailings [J]. *Conservation and Utilization of Mineral Resources*, 2025.
- [2] Gao, L., Tian, S., Zhang, Z., et al. Research progress on comprehensive utilization of molybdenum tailings resources [J]. *Journal of Jilin University (Earth Science Edition)*, 2024, 54(5): 1544-1557.
- [3] Yuan, L., Wang, X., Qi, M., et al. Research progress on the preparation of adsorbent materials from mine tailings [J]. *Conservation and Utilization of Mineral Resources*, 2025.
- [4] Figueiredo, A.S., Bezerra, A.C.S., Costa, L.C.B., et al. Sand mining tailings as supplementary cementitious material [J]. *Buildings*, 2024, 14(8): 2408.
- [5] Zhang, C., Feng, Y., Liu, G., et al. New research progress on the resource utilization of tailings in environmental protection and building materials [J]. *China Mining Magazine*, 2024, 33(11): 5-17.
- [6] Yang, P., Fan, M., Li, W., et al. Feasibility study and environmental cost-benefit analysis of self-compacting concrete with molybdenum tailings [J]. *Bulletin of the Chinese Ceramic Society*, 2025, 44(2): 540-549.
- [7] Zhang, R., Kou, Q., An, G. Research progress on comprehensive utilization of molybdenum tailings [J]. *Multipurpose Utilization of Mineral Resources*, 2024, 46(2): 8-16+51.
- [8] Hu, S., Xiong, X., Li, X., et al. Characterization and utilization potential of typical molybdenum tailings in Shaanxi Province, China [J]. *Environmental Geochemistry and Health*, 2024, 46(8): 265.
- [9] Li, J., Yang, Z., Su, Q., et al. Early hydration and mechanical performance of composited cementitious system prepared from high temperature calcined molybdenum tailings [J]. *Case Studies in Construction Materials*, 2024, 21: e03792.
- [10] Gu, X., Wang, Y., Sun, D., et al. Macro and micro characteristics of slag-steel slag cementitious system under the action of composite activator [J]. *Coal Science and Technology*, 2025.
- [11] Shan, J., Zhang, Z., Gao, P., et al. Study on properties of desulfurized building gypsum modified by inorganic cementitious materials [J]. *Bulletin of the Chinese Ceramic Society*, 2024, 43(1): 268-275.
- [12] Jin, S., Wang, X., Wu, Y. Study on stabilization of clay using slag-desulfurization gypsum-carbide slag binder [J]. *Journal of Engineering Geology*, 2023, 31(2): 397-408.
- [13] Yang, G., Li, C., Xie, W., et al. Effect of carbide slag and steel slag as alkali activators on the key properties of carbide slag-steel slag-slag-phosphogypsum composite cementitious materials [J]. *Frontiers in Materials*, 2024, 11: 1353004.
- [14] Luo, T., Yi, Y., Liu, F., et al. Early-age hydration and strength formation mechanism of composite concrete using molybdenum tailings [J]. *Case Studies in Construction Materials*, 2022, 16: e01101.

- [15] Yu, X., Nie, M., Meng, W., et al. Study on the applicability of molybdenum tailings powder as admixture for cement-based materials [J]. *China Mining Magazine*, 2024, 33(2): 141-148.
- [16] Wang, Y., Zhuge, Y., Yao, Y. Design and performance analysis of ultra-high performance concrete using fully recycled molybdenum tailings waste [J]. *Construction and Building Materials*, 2025, 473: 140981.
- [17] Cui, S., Fan, K., Yao, Y. Preparation and characterization of quaternary clinker-free cementitious materials containing phosphorus slag, calcium carbide slag, desulfurization gypsum, and metakaolin [J]. *Construction and Building Materials*, 2024, 411: 134602.
- [18] Qi, G., Zhang, Q., Liu, X. Regulation mechanism of desulfurization gypsum on hydration characteristics of calcium aluminate-carbide slag co-activated supersulfated cement [J]. *Bulletin of the Chinese Ceramic Society*, 2025, 44(6).
- [19] Ji, X., Wang, Z., Zhang, H., et al. Optimization design and characterization of slag cementitious composites containing carbide slag and desulfurized gypsum based on response surface methodology [J]. *Journal of Building Engineering*, 2023, 77: 107441.
- [20] Guo, Y., Hu, W., Feng, G., et al. Study on the excitation effect and mechanism of coal gasification slag based on solid waste [J]. *Powder Technology*, 2024, 435: 119460.
- [21] Jiang, T., Deng, Y., Li, H., et al. Rheological properties, mechanical performance and hydration characteristics of alkali-activated lithium slag composite cementitious material [J]. *Bulletin of the Chinese Ceramic Society*, 2025, 44(5): 1767-1778.
- [22] Nie, S., Zhou, J., Xu, M., et al. Research progress of low-carbon cementitious materials [J]. *Materials Reports*, 2024, 38(2): 22050304-22050309.
- [23] Feng, W., Yu, Z., Bao, R., et al. Manufacture of tailings-based cementitious materials: Insights into tailings activation strategies [J]. *Construction and Building Materials*, 2024, 439: 137194.
- [24] Su, Z., Cheng, Y., Liu, Z. Study on macroscopic properties and microscopic characteristics of alkali-activated silicon-manganese slag cementitious materials modified by slag [J]. *Bulletin of the Chinese Ceramic Society*, 2025, 44(4): 1276-1287.
- [25] Yin, Z., Li, R., Lin, H., et al. Analysis of influencing factors of cementitious material properties of lead-zinc tailings based on orthogonal tests [J]. *Materials*, 2022, 16(1): 361.
- [26] Lin, H., Yin, Z., Li, S. Optimization of cementitious material with thermal-activated lead-zinc tailings based on response surface methodology [J]. *Materials*, 2024, 17(12): 2926.
- [27] Zhou, Y., Xie, L., Kong, D., et al. Research on optimizing performance of desulfurization-gypsum-based composite cementitious materials based on response surface method [J]. *Construction and Building Materials*, 2022, 341: 127874.
- [28] Fode, T.A., Jande, Y.A.C., Kivevele, T. Modelling and optimization of multiple replacement of supplementary cementitious materials for cement composite by response surface method [J]. *Cleaner Engineering and Technology*, 2024, 19: 100735.
- [29] Song, B., Huang, J., Yang, M., et al. Study on high supplementary cementitious materials content cement: Design and analysis based on response surface method [J]. *Construction and Building Materials*, 2025, 467: 140398.
- [30] Li, Y., Duan, S., Wu, H., et al. Mechanical properties and hydration mechanism of red mud-fly ash-carbide slag composite cementitious material [J]. *Bulletin of the Chinese Ceramic Society*, 2025, 44(3): 1041-1049.
- [31] Wang, C., Ye, P., Zhang, K., et al. Preparation and hydration mechanism of molybdenum tailings composite cementitious material [J]. *Metal Mine*, 2020(9): 41-47.